

Implications of an extended dark energy model with massive neutrinos

RAVI KUMAR SHARMA,¹ KANHAIYA LAL PANDEY,¹ AND SUBINOY DAS¹

¹*Indian Institute of Astrophysics, Bengaluru, Karnataka 560034, India*

ABSTRACT

Recently there has been reports of finding a lower bound on the neutrino mass parameter (Σm_ν) when using ACT and SPTpol data however these bounds on the Σm_ν are still weaker for most case around at 1σ level. In this context, here in this work, we study the consequences of using an enlarged four parameter dynamical dark energy equation of state on neutrino mass parameter as well as on the Hubble and S8 tensions. The four parameter dark energy equation of state incorporates a generic non-linear monotonic evolution of the dark energy equation of state, where the four parameters are the early and the present value of the equation of state, the transition scale factor and the sharpness of the transition. We report that with lensing-marginalized Planck + BAO + Pantheon and prior on absolute magnitude M_B and KIDS/Viking S_8 prior, the model favours a non-zero value for the neutrino mass parameter at the most at 1σ level ($\Sigma m_\nu = 0.1847^{+0.0698}_{-0.165}$ eV). In this case this model also brings down the Hubble tension to 2.5σ level and the S8 tension to $\sim 1.5\sigma$ level. This model also provide a tighter constraints on the value of the dark energy equation of state at present epoch w_0 ($w_0 = -0.9901^{+0.0561}_{-0.0766}$) in comparison to the CPL like parameterization.

Keywords: Dynamical dark energy — Massive neutrinos — Hubble tension — S8 tension

1. INTRODUCTION

The observations of type Ia supernovae show that the expansion of the Universe is accelerating. The acceleration requires the Universe to be dominated by an exotic fluid with negative pressure. The simplest explanation for dark energy is the cosmological constant or vacuum energy that explains the acceleration of the Universe. Though the cosmological constant is preferred from cosmological observations yet its theoretical understanding has been questionable Sahni (2002). The other alternatives of the cosmological constant that can act as dark energy are scalar fields such as quintessence field, modified gravity, phantom dark energy Ballardini et al. (2016); Nojiri et al. (2017); Farhang & Khosravi (2021); Braglia et al. (2021). There has not been any observational evidence of such alternatives but it has not been ruled out either. One such model is dynamical dark energy driven by a slowly rolling scalar field. If this is true, then it opens up many new observational windows which may shed light on the fundamental nature of this mysterious component of the Universe.

The other reason to explore beyond the Λ CDM model is the recently emerging and persistent anomalies in present high precision cosmological data. The mismatch between values of Hubble parameter inferred from CMB data and direct measurements is one of them. The SH0ES (Supernovae H0 for Equation of State) team has measured the value of Hubble parameter $H_0 = 73.2 \pm 1.3$ km/s/Mpc using the distance ladder method Riess et al. (2019); Riess et al. (2021). However The Planck 2018 measurement of CMB (Cosmic Microwave Background) has measured the value of Hubble parameter $H_0 = 67.36 \pm 0.54$ km/s/Mpc using Λ CDM model Planck Collaboration et al. (2020). So there is

ravi.sharma@iiap.res.in

kanhaiya.pandey@iiap.res.in

subinoy@iiap.res.in

a 4.2σ discrepancy between both measurements. This mismatch gained significance with various improved precision measurements see, Freedman (2017); Schöneberg et al. (2021); Di Valentino (2021); Di Valentino et al. (2021a,b).

Similarly there is another tension related to the measured value of $S_8 \equiv \sigma_8(\Omega_m/0.3)^{0.5}$, where σ_8 is the root mean square of matter fluctuations on a $8 h^{-1}\text{Mpc}$ scale, and Ω_m is the total matter abundance. The latest prediction from Planck CMB data within the ΛCDM framework is $S_8 = 0.832 \pm 0.013$ Planck Collaboration et al. (2020).

Originally, observations of galaxies through weak lensing by the CFHTLenS collaboration have indicated that the ΛCDM model predicts a S_8 value that is larger than the direct measurement at the 2σ level Heymans et al. (2013); MacCrann et al. (2015). This tension has since then been further established within the KiDS/Viking data Hildebrandt et al. (2020); Joudaki et al. (2020), but is milder within the DES data Abbott et al. (2018). However, a re-analysis of the DES data, combined with KiDS/Viking, leads to a determination of S_8 that is discrepant with Planck at the 3σ level, $S_8 = 0.755^{+0.019}_{-0.021}$ Joudaki et al. (2020). Recently, the combination of KiDS/Viking and SDSS data has established $S_8 = 0.766^{+0.02}_{-0.014}$ Heymans et al. (2021). However, a study in Nunes & Vagnozzi (2021) shows fainter S_8 tension when redshift-space distortions (RSD) data is included.

There has been a wide range of solutions proposed to solve these cosmological tensions which requires new physics/modifications in the early Universe i.e. pre-recombination era as well as in the late Universe. Not a single model yet fully solves both H_0 and S_8 tensions simultaneously. The class of solutions which invokes modifications of the late-time Universe dynamics in dark energy generally leaves r_s unaffected by construction and has been studied extensively in recent times. The higher value of H_0 is then accommodated by a smaller value of Ω_{DE} or Ω_m at redshift below z_* such that $d_A(z_*)$ stays unaffected as well. This can be done for instance by invoking variations in the dark-energy equation of state Poulin et al. (2018); Bhattacharyya et al. (2019); Poulin et al. (2018); Di Valentino et al. (2017, 2016b, 2015); Poulin et al. (2019); Gogoi et al. (2021); Visinelli et al. (2019); Vagnozzi (2020); Hazra et al. (2022) or decaying dark matter Pandey et al. (2020) Poulin et al. (2016) Abellán et al. (2021b) or non-thermal dark matter Das et al. (2021) with certain level of success.

The study of the dynamical behavior of dark energy is often done in terms of its equation of state $w(z) = \frac{P(z)}{\rho(z)}$ that can vary as a function of redshift. Equation of state $w = -1$ corresponds to the cosmological constant. There are some recent studies where it has been shown that solving of H_0 and S_8 tensions require $w(z) < -1$ at some $z > 0$ and time-varying dark energy equation of state which cross the phantom barrier Heisenberg et al. (2022). Also it has been shown that a large class of quintessence ($w > -1$) models including the ones which arise from string swampland conjecture lower the H_0 parameter and thereby makes H_0 tension worse Banerjee et al. (2021), however, interacting DE models, for example Das et al. (2006) where the variation in $w(z)$ starts from a higher redshift might indeed alleviate the H_0 anomaly. From observations, it's required that equations of state at present time should be consistent with value $w \approx -1$, however, constraints on the equation of state at higher redshift are weaker. There have already been several efforts to parameterize the equation of state of dark energy. Some recent works in this direction can be found in Durrive et al. (2018); Martins & Colomer (2018); Marcondes & Pan (2017); Yang et al. (2021b); Colgáin et al. (2021); Chevallier & Polarski (2001); Linder (2003); Jassal et al. (2005); Efstathiou (1999); Barboza & Alcaniz (2008); Li & Shafieloo (2019); Yang et al. (2021a); Jaber & de la Macorra (2018); Roy et al. (2022); Heisenberg et al. (2022); Theodoropoulos & Perivolaropoulos (2021); Mawas et al. (2021); Anchordoqui et al. (2021); Bamba et al. (2012).

We explore in detail the possibility of dynamical DE with a more general model-independent approach where we go beyond the CPL (Chevalier-Polarski and Linder) parameterization Linder (2003); Chevallier & Polarski (2001) where the dark energy equation of state w evolves linearly with expansion factor a . To be specific, in this paper, we study a generic non-linearly evolving equation of state. Some of the recent works on dynamical dark energy scenario such as Colgáin et al. (2021) suggest that CPL parameterization is not sensitive at low redshifts and thus provide motivation for going beyond CPL like parameterization. It was recently pointed out that if late-time cosmology is modified through time-varying w , one indeed should use the direct prior on the absolute magnitude of supernovae, M_B instead of H_0 prior Lemos et al. (2019); Benevento et al. (2020); Camarena & Marra (2021); Efstathiou (2021). To our knowledge, this work is the first work where we present a detailed analysis of a four parameter dynamical DE model. To do so, we use a generic four parameter model of dynamical dark energy equation of state w originally proposed in Corasaniti & Copeland (2003) and test it against the recent Planck-2018, Pantheon and BAO datasets. In comparison to CPL parameterization, this parameterization has two extra parameters to incorporate the possible non-linear evolution of the equation of state with time. The main interest of this parameterization is that it captures possible transition in the equation of state of the dynamical dark energy during the course of its evolution, which many quintessence/K-essence and phantom dark energy models exhibit Corasaniti & Copeland (2003).

Earlier studies have shown that the total neutrino mass parameter Σm_ν show significant amount of degeneracy with other cosmological parameters (eg., with the matter density parameter Ω_m and the Hubble parameter H_0) if we just use the CMB data alone. Moreover models with a variable $w(z)$, the constraint from CMB is essentially on one number that is the effective equation of state w_{eff} (Jassal et al. 2010). Adding a low redshift measurement data such as the BAO and the SNe data can help in breaking these degeneracies (Di Valentino et al. 2016a; Sutherland 2018) and thus getting a better constraints on the Σm_ν and the DE parameters.

In this study , we find that all four parameters of the equation of state can not be constrained fully with current observational data. Especially, Planck 2018 data alone has poor constraining ability on dark energy parameters. Once we include the BAO and Pantheon data, the constraints improve and the Hubble tension comes down to 2.5σ level from SH0ES measurement and S_8 tension comes down to 1.5σ from KIDS/Viking measurement.

An important aspect of this paper is to get neutrino mass constraints in the 4pDE model. Standard massive neutrinos play an important role in the evolution of the Universe, they leave a non-negligible impact on the cosmic microwave background (CMB) and large-scale structure (LSS) at different epochs of the evolution of the Universe. This impact is used to get a bound on neutrino mass. Some of the effects of standard model neutrinos and dark energy are the same during specific cosmic time. Therefore nature of dark energy has an important role in constraining neutrino mass. Some of the relevant studies we find in the literature are Hannestad (2005) Lorenz et al. (2017) Calabrese et al. (2011) Di Valentino & Melchiorri (2021) Poulin et al. (2018) Vagnozzi et al. (2018) Vagnozzi et al. (2017) Abellán et al. (2021a). In our analysis, we detect a non-zero neutrino mass at 1σ level ($\Sigma m_\nu \sim 0.2 \pm 0.1$ eV) but consistent with zero at 2σ level unlike a previous study Poulin et al. (2018) where the analysis was done with earlier (2015) Planck data and the neutrino mass Σm_ν was found to be non-zero even at $\gtrsim 2\sigma$.

The plan of the paper is as follows. A brief description of the four parameter dynamical dark energy equation of state, $w_{\text{de}}(a)$, is given in section II. In Section III and IV we provide a detailed description of our analysis and results. Then Section V summarizes the paper and future outlook.

2. FOUR-PARAMETER MODEL FOR DARK ENERGY

To investigate the effect of a non-linearly evolving dark energy equation of state, we use a model independent, 4 parameter dynamical dark energy equation of state $w_{\text{de}}(a)$, suggested by Corasaniti & Copeland (2003),

$$w_{\text{de}}(a) = w_0 + (w_m - w_0) \times \Gamma(a) \quad (1)$$

where w_0 and w_m are 2 parameters denoting the initial and final values of the dark energy equation of state, ie., $w_0 = w_{\text{de}}(a = 1)$ and $w_m = w_{\text{de}}(a \ll 1)$. The factor $\Gamma(a)$ contains the other 2 parameters describing the course of the evolution of $w_{\text{de}}(a)$, and is given as,

$$\Gamma(a) = \frac{1 - \exp(-(a - 1)/\Delta_{\text{de}})}{1 - \exp(1/\Delta_{\text{de}})} \times \frac{1 + \exp(a_t/\Delta_{\text{de}})}{1 + \exp(-(a - a_t)/\Delta_{\text{de}})} \quad (2)$$

where a_t is the scale factor at which the transition from w_m to w_0 takes place and the Δ_{de} is the steepness of the transition.

The factor $\Gamma(a)$ in Eq. 1, characterizes the course of the evolution of $w_{\text{de}}(a)$. Figure 1 elaborates the nature of the parameters a_t and Δ_{de} . It can be easily shown that for the two extreme limits of Δ_{de} Eq. 1 takes the following form,

$$\lim_{\Delta_{\text{de}} \rightarrow \infty} w_{\text{de}}(a) = w_0 + (w_m - w_0) \times (1 - a) \quad (3)$$

$$\lim_{\Delta_{\text{de}} \rightarrow 0} w_{\text{de}}(a) = w_0 + \Theta(a_t - a) \times (w_m - w_0) \quad (4)$$

ie., Equation 1 approaches to standard 2 parameter parameterization with $w_a = w_m - w_0$ in the limit of $\Delta_{\text{de}} \rightarrow \infty$ as this is also evident from the green-dashed plot in the Figure 1. Also when $\Delta_{\text{de}} \rightarrow 0$ the function $\Gamma(a)$ tend to become a step function (Heaviside function, Θ) around $a = a_t$ (the orange-dotted plot in the Figure 1).

Our parameterization is generic to a class of non-interacting scalar field dynamical dark energy models only, ie., we assume $c_{s,\text{de}}^{\text{eff}} = 1$. Also this parameterization can only mimic monotonically evolving dynamical dark energy models.

We will consider a homogeneous and isotropic flat background for the universe described by a FLRW metric. If we neglect the radiation density today, Friedmann equation will have the following form,

$$\frac{H^2}{H_0^2} = \Omega_M/a^3 + \Omega_{\text{DE}} \exp \left(3 \times \int_1^a \frac{1 + w_{\text{de}}(a')}{a'} da' \right) \quad (5)$$

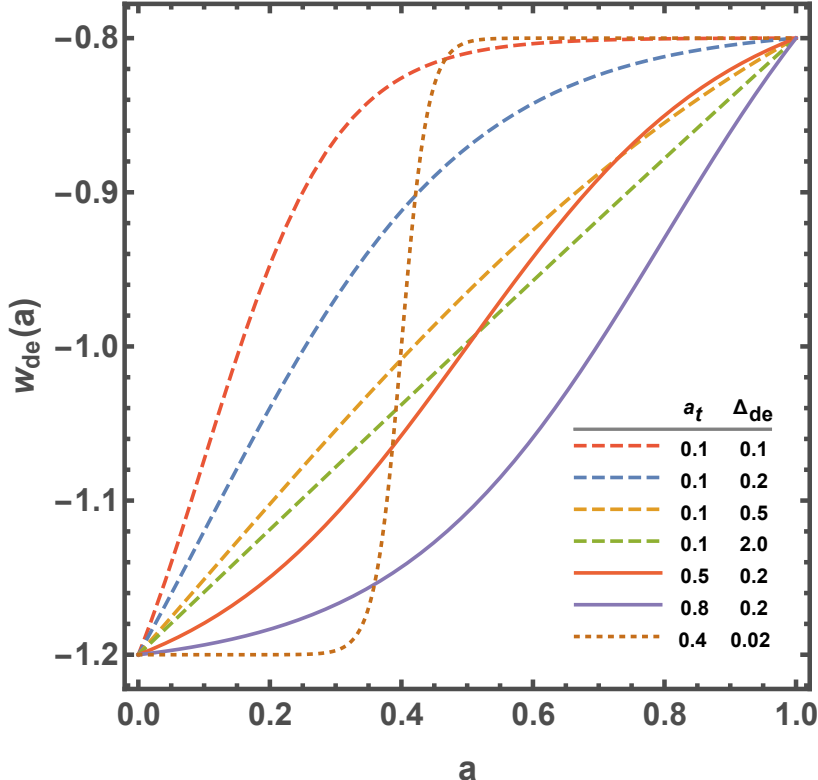


Figure 1. Evolution of w_{de} for different sets of values for a_t and Δ_{de} , parameters w_0 and w_m are fixed to -0.8 and -1.2 respectively.

where Ω_M and Ω_{DE} is matter density and dark energy density parameters respectively and for a flat universe $\Omega_{DE} + \Omega_M = 1$.

2.1. Effect on various cosmological observables

2.1.1. Effect on CMB

Though the dark energy energy starts to dominate the energy content of the universe at late times but still it can affect the CMB data in two ways, one is by affecting the angular diameter distance and the second is through Integrated Sachs Wolfe (ISW) effect. The change in the angular diameter distance is reflected in shifts in the location of the peaks in CMB angular power spectra. On the other hand the late time ISW is sensitive to the low ℓ regime of the CMB angular power spectra. Figure 2 shows the effect of the individual dark energy parameters (w_0 , w_m , a_t , Δ_{de}) on the CMB temperature angular power spectrum while keeping the other parameters fixed.

2.1.2. Effect on BAO

We know the BAO scale can act as a standard ruler. This scale can be used to measure the angular diameter distance, $d_A(z) = c/(1+z) \int_0^z 1/H(z') dz'$, using clustering of galaxies perpendicular to the line of sight and expansion rate $H(z)$ of the universe using clustering along line of sight. Adjustments in cosmological parameters can alter the clustering scale of the galaxies which is related to the sound horizon $r_d = \int_{z_d}^{\infty} c_s(z)/H(z) dz$, where c_s is the sound speed and z_d is the drag epoch. Effectively, BAO measurements actually constrain the combination $r_d * H(z)$ or $d_A(z)/r_d$. Another important observable in redshift surveys is $f\sigma_8$ which is defined as combination of growth rate $f(a)$ and the root mean square normalization of the matter power spectrum σ_8 ,

$$f\sigma_8(a) = a \frac{\delta'_m(a)}{\delta_m(1)} \sigma_{8,0}$$

Figure 7 and Figure 8 in Appdendix respectively show the effect of the individual dark energy parameters (w_0 , w_m , a_t , Δ_{de}) on the quantities $r_d \times H(z)/(1+z)$ and $f(z) \times \sigma_8(z)$ while keeping the other parameters fixed.

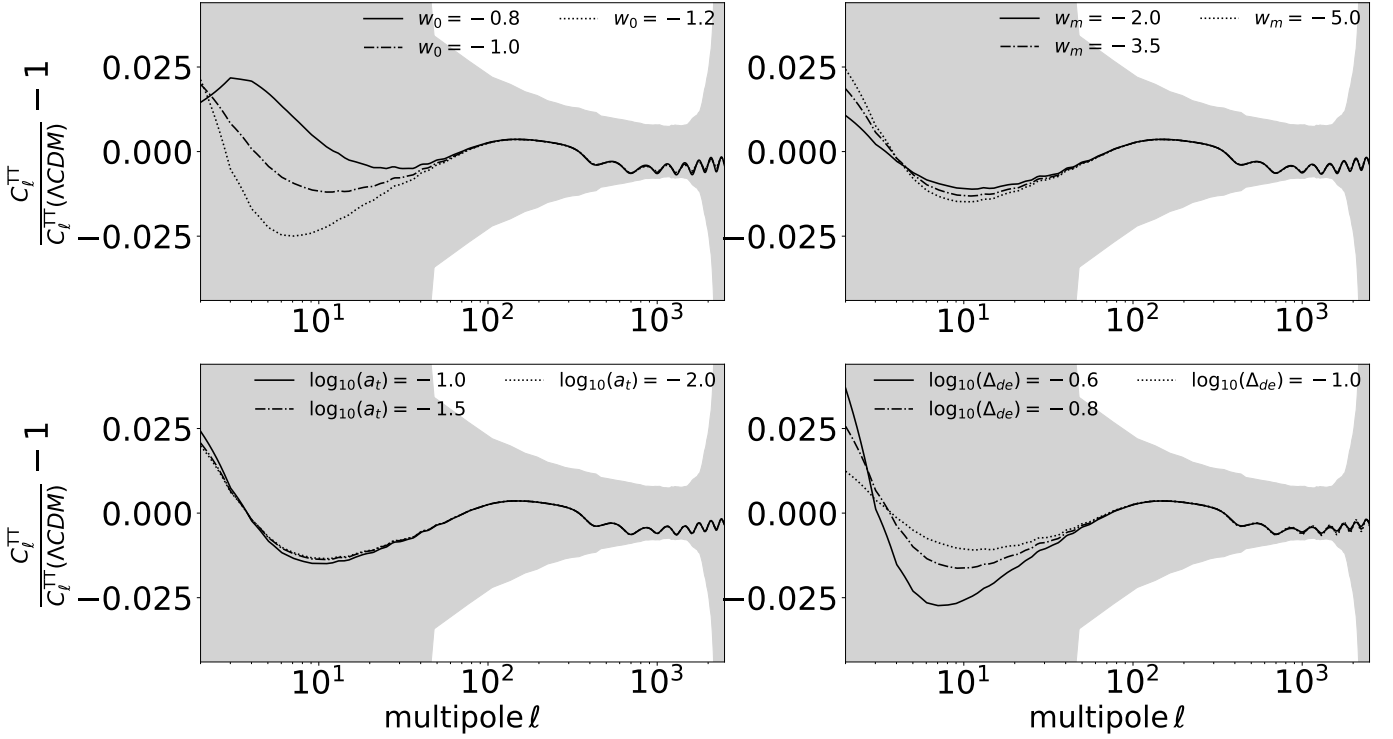


Figure 2. The residual plots of CMB TT power spectra for 4pDE model with respect to Λ CDM model. The shaded region is the Planck 2018 1σ uncertainties. Each of four panels shows effect of varying different dark energy equation of state parameter (see the legends) while fixing other EoS parameters to values ($w_0 = -1.03$, $w_m = -3.97$, $\log_{10}(a_t) = -1.63$, $\log_{10}(\Delta_{de}) = -0.87$).

2.1.3. Supernovae Ia data

SNe data provide geometric constraints for dark energy evolution. These constraints are obtained by comparing the predicted luminosity distance to the SNe with the observed ones. The theoretical model and observations are compared with the measured luminosities,

$$M = m - 5 \log_{10} \left(\frac{d_L}{10} \right)$$

where M is absolute magnitude of the SNe, m is apparent magnitude of the SNe and $d_L = c (1+z) \int_0^z 1/H(z') dz'$ is their luminosity distance in parsec. This depends on the evolution of dark energy through $H(z)$. Figure 9 show the effect of the individual dark energy parameters (w_0 , w_m , a_t , Δ_{de}) on $d_L(z)$ while keeping the other parameters fixed.

3. DETAILS OF ANALYSIS

3.1. Data Sets

- Planck 2018 measurements of the low- ℓ CMB TT, EE, and high- ℓ TT, TE, EE power spectra, together with the gravitational lensing potential reconstruction [Planck Collaboration et al. \(2020\)](#).
- The BAO measurements from 6dFGS at $z = 0.106$ [Beutler et al. \(2011\)](#), SDSS DR7 at $z = 0.15$ [Ross et al. \(2015\)](#), BOSS DR12 at $z = 0.38, 0.51$ and 0.61 [Alam et al. \(2017\)](#), and the joint constraints from eBOSS DR14 Ly- α auto-correlation at $z = 2.34$ [de Sainte Agathe et al. \(2019\)](#) and cross-correlation at $z = 2.35$ [Blomqvist et al. \(2019\)](#).
- The measurements of the growth function $f\sigma_8(z)$ (FS) from the CMASS and LOWZ galaxy samples of BOSS DR12 at $z = 0.38, 0.51$, and 0.61 [Alam et al. \(2017\)](#).
- The Pantheon SNIa catalogue, spanning redshifts $0.01 < z < 2.3$ [Scolnic et al. \(2018\)](#).

Parameter	Prior
w_0	[-5,-0.5]
w_m	[-5,0.5]
$\log(a t_{\text{de}})$	[-3,0]
$\log(\Delta_{\text{de}})$	[-1,0]
Σm_ν	[0,5]

Table 1. List of parameter priors for the additional parameters. Priors for the standard base parameters $\{\omega_b, \omega_{\text{cdm}}, 100 \times \theta_s, n_s, \ln(10^{10} A_s), \tau_{\text{reio}}\}$ are kept same as the default set into the MontePython-v3 (Thejs Brinckmann 2018) code.

Data-set ↓	$\nu 4\text{pDE}$			
	I	II	III	IV
Planck high- ℓ TT,TE,EE	2345.70	2347.49	2347.84	2349.06
Planck low- ℓ EE	396.31	395.78	396.16	396.90
Planck low- ℓ TT	23.56	22.87	22.86	22.76
Planck lensing	8.84	8.95	8.70	9.37
Pantheon	1026.90	1027.22	1027.89	1027.93
BAO FS BOSS DR12	7.15	7.18	8.52	9.96
BAO BOSS low- z	1.63	2.68	3.245	3.47
absolute M	—	13.05	10.43	—
SHOES	—	—	—	9.865
S8	—	—	4.717	2.15
Total	3810.13	3825.18	3830.39	3831.50

Table 2. Best-fit χ^2 per experiment (and total) in the $\nu 4\text{pDE}$ model. The column headings in Roman-numeral correspond to different data/prior-combinations as, I) Planck+Ext ; II) Planck+Ext+MB ; III) Planck+Ext+MB+S8; IV) Planck+Ext+H0+S8.

- The SH0ES result, modeled with a Gaussian likelihood centered on $H_0 = 73.2 \pm 1.3 \text{ km/s/Mpc}$ Riess et al. (2021); however, choosing a different value that *combines* various direct measurements would not affect the result, given their small differences.
- The KIDS1000+BOSS+2dLenS weak lensing data, compressed as a split-normal likelihood on the parameter $S_8 = 0.766^{+0.02}_{-0.014}$ Heymans et al. (2021).
- The Gaussian prior on absolute magnitude $M_B = -19.244 \pm 0.037 \text{ mag}$ Camarena & Marra (2021) , corresponding to the SN measurements from SH0ES.

3.2. Methodology

Our baseline cosmology consists in the following combination of the six Λ CDM parameters $\{\omega_b, \omega_{\text{cdm}}, 100 \times \theta_s, n_s, \ln(10^{10} A_s), \tau_{\text{reio}}\}$, plus four dark energy equation of state parameters as discussed in Section 2, namely w_0 , w_m , a_t , Δ_{de} and neutrino mass Σm_ν . We dub this model as $\nu 4\text{pDE}$. We run MCMC analysis of $\nu 4\text{pDE}$ model against various combinations of the CMB, BAO and supernovae data sets (details of which is given in Section 3.1) with the Metropolis-Hastings algorithm as implemented in the MontePython-v3 (Thejs Brinckmann 2018) code interfaced with our modified version of CLASS. We use the prior ranges for $\nu 4\text{pDE}$ model as given in the Table 1, priors for the other six base parameters $\{\omega_b, \omega_{\text{cdm}}, 100 \times \theta_s, n_s, \ln(10^{10} A_s), \tau_{\text{reio}}\}$ are kept same as the default set into the MontePython-v3 (Thejs Brinckmann 2018) code. All reported χ^2_{min} are obtained with the python package iMINUIT¹ James & Roos (1975). We make use of a Choleski decomposition to better handle the large number of nuisance parameters Lewis et al. (2000) and consider chains to be converged with the Gelman-Rubin convergence criterion $R - 1 < 0.05$ Gelman & Rubin (1992). We also run MCMC chains for the standard Λ CDM and ν CPL (CPL parameterization with neutrino mass as free parameter) models with different combinations of data sets and priors for making comparisons.

¹ <https://iminuit.readthedocs.io/>

Parameter	ν pDE			
	Planck+Ext	Planck+Ext+ M_B	Planck+Ext+ M_B+S_8	Planck+Ext+ H_0+S_8
$100 \omega_b$	$2.231(2.235)^{+0.01423}_{-0.01359}$	$2.235(2.247)^{+0.01554}_{-0.01479}$	$2.239(2.249)^{+0.0155}_{-0.0148}$	$2.238(2.239)^{+0.015}_{-0.015}$
ω_{cdm}	$0.1202(0.1202)^{+0.00108}_{-0.0010613}$	$0.1200(0.1185)^{+0.0010481}_{-0.0010872}$	$0.1193(0.1191)^{+0.00105}_{-0.00109}$	$0.1194(0.1192)^{+0.0011}_{-0.001}$
$100 * \theta_s$	$1.0418(1.0417)^{+0.00028}_{-0.0003067}$	$1.0419(1.0419)^{+0.0003093}_{-0.0002733}$	$1.0419(1.0419)^{+0.000309}_{-0.00273}$	$1.042(1.04198)^{+0.00029}_{-0.00028}$
n_s	$0.9631(0.9642)^{+0.0038948}_{-0.004134}$	$0.9636(0.9679)^{+0.00400}_{-0.0042631}$	$0.9647(0.9652)^{+0.004}_{-0.00426}$	$0.9645(0.9644)^{+0.0042}_{-0.0042}$
$\ln(10^{10} A_s)$	$3.043(3.047)^{+0.0150}_{-0.0147}$	$3.042(3.037)^{+0.01488}_{-0.014812}$	$3.042(3.040)^{+0.0149}_{-0.0148}$	$3.042(3.0469)^{+0.015}_{-0.016}$
τ_{reio}	$0.0537(0.0555)^{+0.007626}_{-0.007351}$	$0.05357(0.05308)^{+0.0072268}_{-0.007737}$	$0.05436(0.05511)^{+0.00723}_{-0.00754}$	$0.054(0.0577)^{+0.0076}_{-0.0079}$
Σm_ν [eV]	$0.1129(0.038)^{+0.0276}_{-0.1129}$	$0.1069(0.0094)^{+0.0697}_{-0.1069}$	$0.1847(0.1043)^{+0.0698}_{-0.165}$	$0.1857(0.2748)^{+0.091}_{-0.13}$
w_0	$-0.9856(-1.038)^{+0.053}_{-0.065}$	$-0.9886(-1.011)^{+0.053}_{-0.073}$	$-0.9901(-1.029)^{+0.0561}_{-0.0766}$	$-1.04(-0.9446)^{+0.049}_{-0.062}$
w_m	$-2.285(-1.040)^{+1.5}_{-0.59}$	$-2.715(-1.611)^{+1.6}_{-0.91}$	unconstrained	$-2.45(-3.1)^{+1.4}_{-0.78}$
$\log_{10}(a_t)$	unconstrained	unconstrained	unconstrained	unconstrained
$\log_{10}(\Delta_{\text{de}})$	$-0.6752(-0.7649)^{+0.066}_{-0.32}$	$-0.6687(-0.9264)^{+0.065}_{-0.33}$	$-0.6313(-0.8739)^{+0.0809}_{-0.368}$	$-0.6936(-0.4452)^{+0.068}_{-0.31}$
M_B	$-19.40(-19.40)^{+0.01887}_{-0.01962}$	$-19.37(-19.37)^{+0.01629}_{-0.01655}$	$-19.369(-19.359)^{+0.01580}_{-0.01615}$	$-19.37(-19.36)^{+0.017}_{-0.015}$
σ_8	$0.8135(0.8279)^{+0.01685}_{-0.01203}$	$0.8225(0.8216)^{+0.01658}_{-0.01303}$	$0.8073(0.8206)^{+0.01763}_{-0.01462}$	$0.8093(0.7966)^{+0.017}_{-0.014}$
Ω_m	$0.3064(0.3038)^{+0.00779}_{-0.00810}$	$0.2973(0.2954)^{+0.0069}_{-0.0074}$	$0.294(0.2893)^{+0.00637}_{-0.00654}$	$0.2919(0.2955)^{+0.006}_{-0.0064}$
S_8	$0.822(0.832)^{+0.0170}_{-0.0117}$	$0.8188(0.81)^{+0.016}_{-0.013}$	$0.799(0.8051)^{+0.0163}_{-0.0134}$	$0.7982(0.8043)^{+0.014}_{-0.013}$
H_0 [km/s/Mpc]	$68.21(68.53)^{+0.846}_{-0.823}$	$69.22(69.14)^{+0.843}_{-0.791}$	$69.44(69.87)^{+0.697}_{-0.724}$	$69.71(69.58)^{+0.7}_{-0.7}$
χ^2_{min}	3810.13	3825.18	3830.34	3831.50
$\Delta\chi^2_{\text{min}}$	-1.4	-6.53	-5.5	-4.3

Table 3. The mean (best-fit) $\pm 1\sigma$ error of the cosmological parameters reconstructed from the lensing-marginalized Planck+BAO+SN1a data and combinations of M_B and S_8 priors for ν pDE model. We also report the corresponding $\Delta\chi^2_{\text{min}}$ values.

Parameter	ν CPL			
	Planck+Ext	Planck+Ext+ M_B	Planck+Ext+ S_8+M_B	Planck+Ext+ S_8+M_B
$100 \omega_b$	$2.2334(2.23425)^{+0.01460}_{-0.01418}$	$2.2364(2.2461)^{+0.01429}_{-0.01442}$	$2.239(2.2291)^{+0.015}_{-0.015}$	$2.239(2.2291)^{+0.015}_{-0.015}$
ω_{cdm}	$0.12016(0.1197)^{+0.001131}_{-0.001073}$	$0.1201(0.1196)^{+0.0011}_{-0.0011}$	$0.1194(0.1189)^{+0.0011}_{-0.0011}$	$0.1194(0.1189)^{+0.0011}_{-0.0011}$
$100 * \theta_s$	$1.0419(1.197716)^{+0.0002927}_{-0.0003023}$	$1.042(1.04173)^{+0.0003}_{-0.00028}$	$1.042(1.0418)^{+0.00028}_{-0.00031}$	$1.042(1.0418)^{+0.00028}_{-0.00031}$
$\ln(10^{10} A_s)$	$3.0448(1.197716)^{+0.01478}_{-0.01570}$	$3.043(3.0378)^{+0.015}_{-0.015}$	$3.041(3.0268)^{+0.015}_{-0.015}$	$3.041(3.0268)^{+0.015}_{-0.015}$
n_s	$0.96397(0.9657)^{+0.00416}_{-0.00394}$	$0.9641(0.9657)^{+0.0041}_{-0.0041}$	$0.9645(0.9669)^{+0.0041}_{-0.0042}$	$0.9645(0.9669)^{+0.0041}_{-0.0042}$
τ_{reio}	$0.05446(0.05415)^{+0.00752}_{-0.00801}$	$0.05375(0.05149)^{+0.0074}_{-0.0077}$	$0.05388(0.04686)^{+0.0073}_{-0.0074}$	$0.05388(0.04686)^{+0.0073}_{-0.0074}$
Σm_ν [eV]	$0.1092(0.04848)^{+0.0255}_{-0.100}$	$0.09942(0.00578)^{+0.025}_{-0.099}$	$0.1877(0.074)^{+0.094}_{-0.14}$	$0.1877(0.074)^{+0.094}_{-0.14}$
w_0	$-0.9690(-0.99195)^{+0.0787}_{-0.0830}$	$-0.9541(-0.9558)^{+0.076}_{-0.094}$	$-0.9393(-1.08)^{+0.09}_{-0.095}$	$-0.9393(-1.08)^{+0.09}_{-0.095}$
w_a	$-0.2915(-0.1680)^{+0.409}_{-0.292}$	$-0.5008(-0.3023)^{+0.49}_{-0.28}$	$-0.6716(0.0303)^{+0.55}_{-0.39}$	$-0.6716(0.0303)^{+0.55}_{-0.39}$
M_B	$-19.40(-19.3923)^{+0.0191}_{-0.0179}$	$-19.37(-19.374)^{+0.016}_{-0.016}$	$-19.37(-19.376)^{+0.016}_{-0.017}$	$-19.37(-19.376)^{+0.016}_{-0.017}$
σ_8	$0.8134(0.8237)^{+0.0155}_{-0.0120}$	$0.8237(-0.8306)^{+0.016}_{-0.012}$	$0.8061(0.8172)^{+0.018}_{-0.015}$	$0.8061(0.8172)^{+0.018}_{-0.015}$
Ω_m	$0.3074(0.3017)^{+0.00723}_{-0.00808}$	$0.2974(0.2977)^{+0.00664}_{-0.00718}$	$0.2948(0.2860)^{+0.00673}_{-0.00703}$	$0.2948(0.2860)^{+0.00673}_{-0.00703}$
S_8	$0.8233(0.827)^{+0.0156}_{-0.0124}$	$0.820(0.825)^{+0.0152}_{-0.0125}$	$0.798(0.802)^{+0.0157}_{-0.0127}$	$0.798(0.802)^{+0.0157}_{-0.0127}$
H_0 [km/s/Mpc]	$68.09(68.62)^{+0.824}_{-0.768}$	$69.23(69.10)^{+0.740}_{-0.742}$	$69.36(69.71)^{+0.720}_{-0.772}$	$69.36(69.71)^{+0.720}_{-0.772}$
χ^2_{min}	3809.86	3824.43	3833.08	3833.08
$\Delta\chi^2_{\text{min}}$	-1.67	-7.23	-2.76	-2.76

Table 4. The mean (best-fit) $\pm 1\sigma$ error of the cosmological parameters reconstructed from the lensing-marginalized Planck+BAO+SN1a data and combinations of M_B and S_8 priors for ν CPL model. We also report the corresponding $\Delta\chi^2_{\text{min}}$ values.

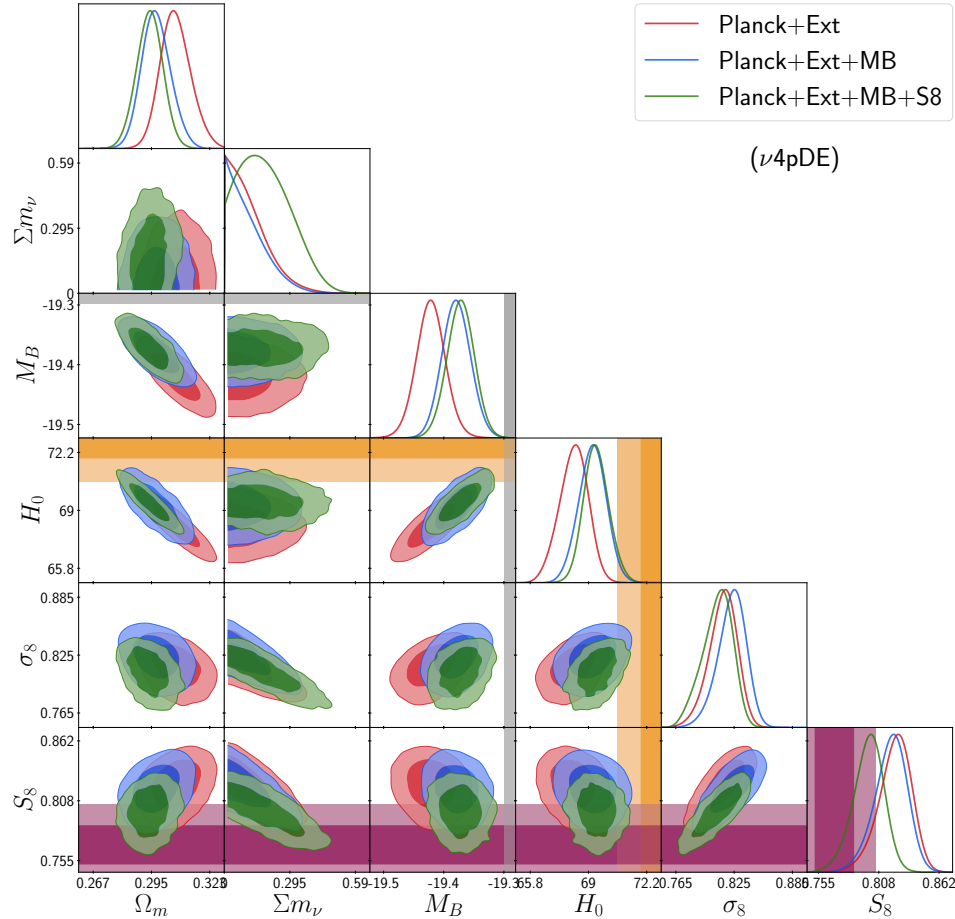


Figure 3. 2D posterior distributions of $(\Omega_m, \Sigma m_\nu, M_B, H_0, \sigma_8, S_8)$ for $\nu 4pDE$ model with Planck+Ext data and different prior combination. We have also added 68% (dark orange) and 95% (light orange) bands corresponding to a H_0 measurement from SH0ES and 68% (dark purple) and 95% (light purple) bands corresponding to S_8 measurement from KIDS1000+BOSS+2dfLenS.

4. RESULTS

We ran three sets of models, the first one is the standard “ Λ CDM Model”. The other two are dynamical dark energy models namely $\nu 4pDE$ and νCPL models model. Each model is constrained with combinations of the data sets, Planck TT, EE, TE+Planck Lensing (see Section 3.1) dubbed as “Planck”, BAO and Pantheon (see Section 3.1), together dubbed as “Ext” and the priors H_0 , M_B and S_8 (see Section 3.1) dubbed as “H0”, “MB” and “S8” respectively. We use the standard Λ CDM model with Planck+Ext dataset as our base model for computing $\Delta\chi^2$ values.

The results of the $\nu 4pDE$ model with combined data sets for various cases are reported in Table 3, the 2D posterior distributions (H_0 , M_B , S_8 and Σm_ν) are shown in Figure 3 and the 1d posterior distributions of the dark energy equation (DE) of state parameters are shown in the Figure 5. The χ^2_{\min} values for this model corresponding to different dataset/prior combinations are reported in Table 2.

We find that w_0 is well constrained for each dataset combination and is consistent with the cosmological constant. However, the other three DE parameters are less constrained or unconstrained. Especially in the case of parameter $\log_{10}(a_t)$ we don't find the lower bound. This is not surprising given the fact the data does not seem to be favoring very sharp transition, i.e., very small value for Δ_{de} , in that case $w_{de}(z)$ has rather weak dependence on the parameter a_t (see Equations 3 and 4) and hence resulting in a weak constraints on the parameter a_t . The overall $\Delta\chi^2_{\min}$ is -1.7 compared to our base Λ CDM model, though we still have the H_0 tension at $\sim 3.2\sigma$ and S_8 tension at $\sim 2.5\sigma$ with this model.

When using the M_B prior, there is no major impact on the equation of state parameters except the values of w_m shift slightly more negative. In this case, the model has H_0 tension at $\sim 2.6\sigma$ with SH0ES results. The overall χ^2_{\min} shift is -6.5 compared to the Λ CDM model.

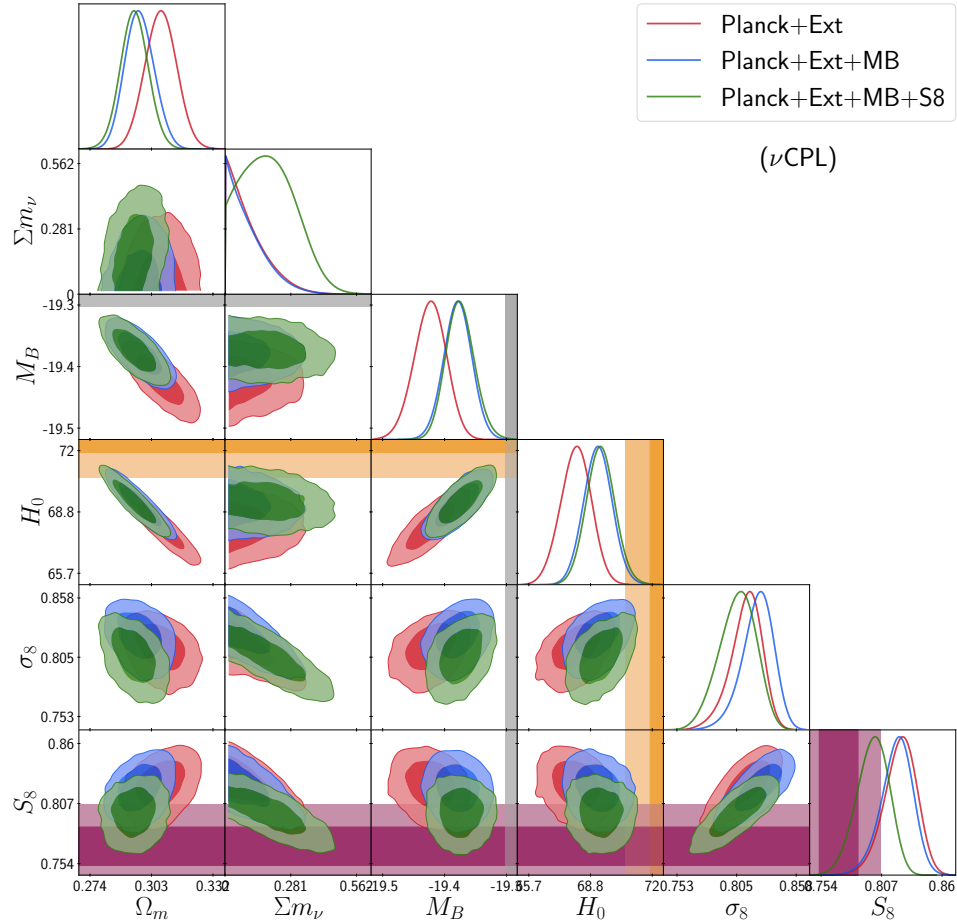


Figure 4. 2D posterior distributions of $(\Omega_m, \Sigma m_\nu, M_B, H_0, \sigma_8, S_8)$ for ν CPL model with Planck+Ext data and different prior combination. We have also added 68% (dark orange) and 95% (light orange) bands corresponding to a H_0 measurement from SH0ES and 68% (dark purple) and 95% (light purple) bands corresponding to S_8 measurement from KIDS1000+BOSS+2dfLenS.

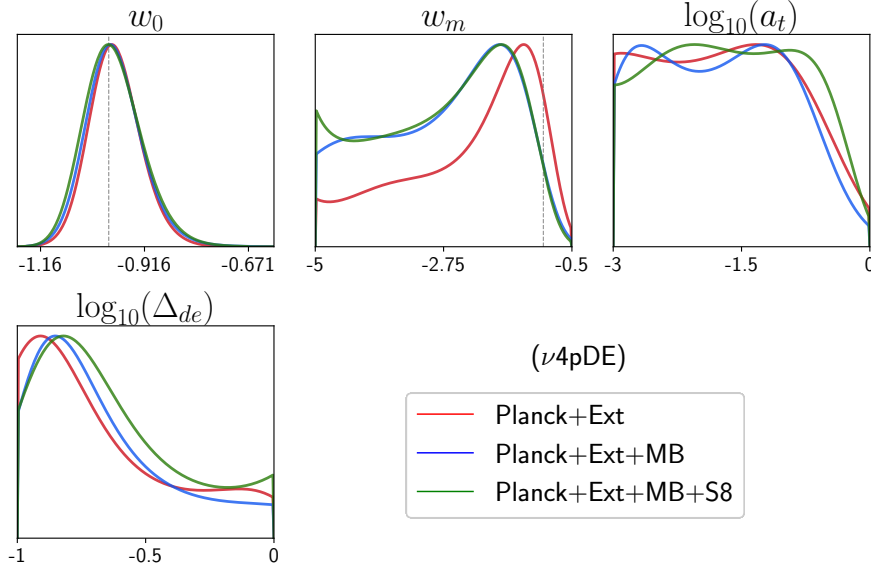


Figure 5. 1D posterior distributions of equation of state parameters $\{w_0, w_m, \log_{10}(a_t), \log_{10}(\Delta_{de})\}$ for ν 4pde model with Planck+Ext data and different prior combinations (see legends).

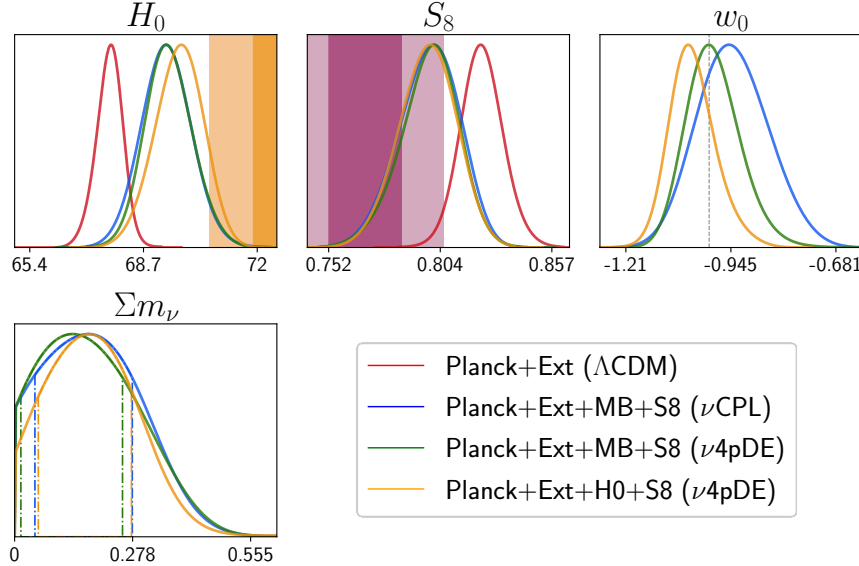


Figure 6. 1D posterior distributions of $(H_0, S_8, w_0, \sum m_\nu)$ for different models and combination of priors (see legends). The dot-dashed vertical lines in the Σm_ν panel correspond to respective 1σ levels.

For the case when M_B and S_8 priors are applied simultaneously, we find that H_0 attains high value, and there is a decrease in S_8 value i.e., we find negative correlation between parameter S_8 and H_0 in this case (see Figure 3). This model brings down the S_8 tension below $\leq 1.5\sigma$ and H_0 tension from $\leq 2.5\sigma$. In this case, we also get a peak in the posterior of the neutrino mass (see Figure 3).

4.1. Comparison between ν CPL Model and the ν 4pDE model

We also run the ν CPL model with same data combinations. Results of this model reported in Table 4 and the 2D posterior distributions are shown in Figure 4. Both the parameters w_0 and w_a are well constrained for ν CPL model. We find the posterior distribution of main cosmological parameters $\{\omega_b, \omega_{\text{cdm}}, 100 \times \theta_s, n_s, \ln(10^{10} A_s), \tau_{\text{reio}}\}$ of this model are matched with the ν 4pDE model. However the model parameters (w_0 and w_a) are different for obvious reasons.

Figure 6 shows a comparison among the ν 4pDE, ν CPL and the base Λ CDM model in terms of the 1d posteriors of parameters $\{H_0, S_8, w_0, \sum m_\nu\}$. The parameter w_0 is constrained more in the ν 4pDE model compare to the ν CPL model. However, when we don't use any prior, we do not notice a significant change in H_0 and S_8 compared to Λ CDM model. But when we use M_B prior, the level of H_0 tension is reduced, and is within 2.5σ level with SH0ES measurement. Similarly, when we add S_8 prior, we notice a slight reduction in the S_8 parameter also.

4.2. Comparison between H_0 prior and the M_B prior

When using the prior on H_0 instead of M_B , the main impact on results is on the parameters w_0 and H_0 . The parameter H_0 attains a slightly higher value compared to M_B prior case and w_0 shifts towards a lower value. The results are compared in Figure 6. This result is true for ν CPL model as well. We also see that H_0 prior supports a non zero neutrino mass more in comparison to the M_B prior. In summary we say that use of H_0 prior has stronger impact on the w_0 , Σm_ν and for obvious reasons on H_0 compared to the case with M_B prior.

5. CONCLUSIONS AND DISCUSSION

We have investigated a generic model of non-linearly evolving dynamical dark energy equation of state w with massive neutrinos (ν 4pDE model), in the light of the recent Planck, Pantheon, BAO data and recent measurements of H_0 and S_8 . We have studied the effect of such parameterization on the background and derived cosmological parameters. The results of our analysis is in accordance with the earlier studies with a linear evolution of w_{de} (CPL like) [Poulin et al. \(2018\)](#); [Di Valentino et al. \(2017, 2016b, 2015\)](#) and a few other parameterization of dynamical dark energy [Zhao et al. \(2017\)](#); [Zhang et al. \(2017\)](#); [Bhattacharyya et al. \(2019\)](#). We do not get any strong constraints on the two

Data →	Planck+Ext+MB		Planck+Ext+MB+S8	
Model ↓	$\Delta\chi^2_{\min}$	ΔAIC	$\Delta\chi^2_{\min}$	ΔAIC
ΛCDM	0	0	0	0
νCPL	-7.23	-1.23	-2.76	+3.24
ν4pDE	-6.53	+3.47	-5.50	+4.50

Table 5. Comparison of $\Delta\chi^2_{\min}$ and ΔAIC for ν4pDE and νCPL models.

extra parameters a_t and Δ_{de} at $\gtrsim 1\sigma$ level, constraints on w_0 are in good agreement with the νCPL parameterization. However, we do get slightly different and a more tightly constrained w_0 when the model is tested against Planck and external data (Pantheon+BAO) put together. The added external prior on parameters M_B and S_8 makes the difference in νCPL and ν4pDE parameterization even broader. The ν4pDE model can bring down the Hubble tension to $\sim 2.5\sigma$ level and the S_8 tension to $\sim 1.5\sigma$ level when tested against Planck, BAO and Pantheon supernovae data together. More importantly, we find that there is a slightly negative correlation between the parameters S_8 and H_0 with ν4pDE model which is very interesting.

However, both the ν4pDE model and νCPL model improves $\Delta\chi^2_{\min}$ for the Planck+Ext dataset and the recent measurements of H_0 and S_8 in comparison to ΛCDM , this lowering of χ^2_{\min} is achieved at the expense of adding extra parameters. So if we follow ΔAIC criteria², the level of success of these models degrades as none of the models has significantly improved ΔAIC value over ΛCDM model. From table 5 it is evident that when considered Planck+Ext+MB, νCPL is still a preferred model. But when we consider Planck+Ext+MB+S8, all the models (4pDE, ν4pDE , νCPL) perform worse in comparison to ΛCDM .

We also see that with added S_8 prior ν4pDE favours a non-zero value for the neutrino mass parameter ($\Sigma m_\nu \sim 0.2 \pm 0.1$ eV), which is in agreement with earlier work using the νCPL parameterization (Poulin et al. 2018) however our analysis does not detect lower bound on Σm_ν parameter at $\gtrsim 1\sigma$. Earlier work such as Poulin et al. (2018) where 2015 Planck data has been used, the neutrino mass Σm_ν was found to be non-zero even at $\gtrsim 2\sigma$. Also in a recent work Di Valentino & Melchiorri (2021) reports a non-zero value for the neutrino mass when used WMAP data along with ACT-DR4 and SPT-3G data. However they also get similar results on Σm_ν as ours when recent Planck and BAO data is used. The well known lensing anomaly in the Planck data ($A_{\text{lens}} \neq 1$) could be playing a role here which needs to be investigated further in more details.

ACKNOWLEDGEMENTS

We thank Vivian Poulin for reading the draft and for his valuable inputs. We thank Pier Stefano Corasaniti, Eoin O Colgain and Sunny Vagnozzi for their valuable inputs. SD and KP acknowledge SERB DST Government of India grant CRG/2019/006147 for supporting the project. We acknowledge HPC NOVA, IIA Bangalore where numerical simulations were performed.

² Akaike Information Criterion (AIC) is one of the popular methods of estimating the relative quality of proposed models for a given data. AIC is based on using a trade-off between the goodness of fit of the model and the simplicity. AIC uses a models log-likelihood as a measure of fit and the number of parameters in the model as the complexity of the model. If N_{Model} is the total number of parameters in a model the AIC score for that model is given by,

$$\Delta\text{AIC} = \chi^2_{\min, \text{Model}} - \chi^2_{\min, \Lambda\text{CDM}} + 2(N_{\text{Model}} - N_{\Lambda\text{CDM}})$$

REFERENCES

- Abbott, T., et al. 2018, Phys. Rev. D, 98, 043526, doi: [10.1103/PhysRevD.98.043526](https://doi.org/10.1103/PhysRevD.98.043526)
- Abellán, G. F., Chacko, Z., Dev, A., et al. 2021a, <https://arxiv.org/abs/2112.13862>
- Abellán, G. F., Murgia, R., & Poulin, V. 2021b, Phys. Rev. D, 104, 123533, doi: [10.1103/PhysRevD.104.123533](https://doi.org/10.1103/PhysRevD.104.123533)
- Alam, S., et al. 2017, Mon. Not. Roy. Astron. Soc., 470, 2617, doi: [10.1093/mnras/stx721](https://doi.org/10.1093/mnras/stx721)
- Anchordoqui, L. A., Di Valentino, E., Pan, S., & Yang, W. 2021, JHEAp, 32, 121, doi: [10.1016/j.jheap.2021.08.001](https://doi.org/10.1016/j.jheap.2021.08.001)
- Ballardini, M., Finelli, F., Umiltà, C., & Paoletti, D. 2016, J. Cosmology Astropart. Phys., 5, 067, doi: [10.1088/1475-7516/2016/05/067](https://doi.org/10.1088/1475-7516/2016/05/067)
- Bamba, K., Capozziello, S., Nojiri, S., & Odintsov, S. D. 2012, Ap&SS, 342, 155, doi: [10.1007/s10509-012-1181-8](https://doi.org/10.1007/s10509-012-1181-8)
- Banerjee, A., Cai, H., Heisenberg, L., et al. 2021, Phys. Rev. D, 103, L081305, doi: [10.1103/PhysRevD.103.L081305](https://doi.org/10.1103/PhysRevD.103.L081305)
- Barboza, Jr., E. M., & Alcaniz, J. S. 2008, Phys. Lett. B, 666, 415, doi: [10.1016/j.physletb.2008.08.012](https://doi.org/10.1016/j.physletb.2008.08.012)
- Benevento, G., Hu, W., & Raveri, M. 2020, Phys. Rev. D, 101, 103517, doi: [10.1103/PhysRevD.101.103517](https://doi.org/10.1103/PhysRevD.101.103517)
- Beutler, F., Blake, C., Colless, M., et al. 2011, Mon. Not. Roy. Astron. Soc., 416, 3017, doi: [10.1111/j.1365-2966.2011.19250.x](https://doi.org/10.1111/j.1365-2966.2011.19250.x)
- Bhattacharyya, A., Alam, U., Lal Pandey, K., Das, S., & Pal, S. 2019, ApJ, 876, 143, doi: [10.3847/1538-4357/ab12d6](https://doi.org/10.3847/1538-4357/ab12d6)
- Blomqvist, M., et al. 2019, Astron. Astrophys., 629, A86, doi: [10.1051/0004-6361/201935641](https://doi.org/10.1051/0004-6361/201935641)
- Braglia, M., Ballardini, M., Finelli, F., & Koyama, K. 2021, Phys. Rev. D, 103, 043528, doi: [10.1103/PhysRevD.103.043528](https://doi.org/10.1103/PhysRevD.103.043528)
- Calabrese, E., Huterer, D., Linder, E. V., Melchiorri, A., & Pagano, L. 2011, Phys. Rev. D, 83, 123504, doi: [10.1103/PhysRevD.83.123504](https://doi.org/10.1103/PhysRevD.83.123504)
- Camarena, D., & Marra, V. 2021, Mon. Not. Roy. Astron. Soc., 504, 5164, doi: [10.1093/mnras/stab1200](https://doi.org/10.1093/mnras/stab1200)
- Chevallier, M., & Polarski, D. 2001, Int. J. Mod. Phys. D, 10, 213, doi: [10.1142/S0218271801000822](https://doi.org/10.1142/S0218271801000822)
- Chevallier, M., & Polarski, D. 2001, International Journal of Modern Physics D, 10, 213, doi: [10.1142/S0218271801000822](https://doi.org/10.1142/S0218271801000822)
- Colgáin, E. O., Sheikh-Jabbari, M. M., & Yin, L. 2021, Phys. Rev. D, 104, 023510, doi: [10.1103/PhysRevD.104.023510](https://doi.org/10.1103/PhysRevD.104.023510)
- Corasaniti, P. S., & Copeland, E. J. 2003, Phys. Rev. D, 67, 063521, doi: [10.1103/PhysRevD.67.063521](https://doi.org/10.1103/PhysRevD.67.063521)
- Das, S., Corasaniti, P. S., & Khouri, J. 2006, Phys. Rev. D, 73, 083509, doi: [10.1103/PhysRevD.73.083509](https://doi.org/10.1103/PhysRevD.73.083509)
- Das, S., Maharana, A., Poulin, V., & Kumar, R. 2021, <https://arxiv.org/abs/2104.03329>
- de Sainte Agathe, V., et al. 2019, Astron. Astrophys., 629, A85, doi: [10.1051/0004-6361/201935638](https://doi.org/10.1051/0004-6361/201935638)
- Di Valentino, E. 2021, Mon. Not. Roy. Astron. Soc., 502, 2065, doi: [10.1093/mnras/stab187](https://doi.org/10.1093/mnras/stab187)
- Di Valentino, E., Giusarma, E., Mena, O., Melchiorri, A., & Silk, J. 2016a, Phys. Rev. D, 93, 083527, doi: [10.1103/PhysRevD.93.083527](https://doi.org/10.1103/PhysRevD.93.083527)
- Di Valentino, E., & Melchiorri, A. 2021, <https://arxiv.org/abs/2112.02993>
- Di Valentino, E., & Melchiorri, A. 2021, arXiv e-prints, arXiv:2112.02993. <https://arxiv.org/abs/2112.02993>
- Di Valentino, E., Melchiorri, A., Linder, E. V., & Silk, J. 2017, Phys. Rev. D, 96, 023523, doi: [10.1103/PhysRevD.96.023523](https://doi.org/10.1103/PhysRevD.96.023523)
- Di Valentino, E., Melchiorri, A., & Silk, J. 2015, Phys. Rev. D, 92, 121302, doi: [10.1103/PhysRevD.92.121302](https://doi.org/10.1103/PhysRevD.92.121302)
- . 2016b, Physics Letters B, 761, 242, doi: [10.1016/j.physletb.2016.08.043](https://doi.org/10.1016/j.physletb.2016.08.043)
- Di Valentino, E., Mena, O., Pan, S., et al. 2021a, Class. Quant. Grav., 38, 153001, doi: [10.1088/1361-6382/ac086d](https://doi.org/10.1088/1361-6382/ac086d)
- Di Valentino, E., et al. 2021b, Astropart. Phys., 131, 102605, doi: [10.1016/j.astropartphys.2021.102605](https://doi.org/10.1016/j.astropartphys.2021.102605)
- Durive, J.-B., Ooba, J., Ichiki, K., & Sugiyama, N. 2018, Phys. Rev. D, 97, 043503, doi: [10.1103/PhysRevD.97.043503](https://doi.org/10.1103/PhysRevD.97.043503)
- Efstathiou, G. 1999, Mon. Not. Roy. Astron. Soc., 310, 842, doi: [10.1046/j.1365-8711.1999.02997.x](https://doi.org/10.1046/j.1365-8711.1999.02997.x)
- Efstathiou, G. 2021, MNRAS, 505, 3866, doi: [10.1093/mnras/stab1588](https://doi.org/10.1093/mnras/stab1588)
- Farhang, M., & Khosravi, N. 2021, Phys. Rev. D, 103, 083523, doi: [10.1103/PhysRevD.103.083523](https://doi.org/10.1103/PhysRevD.103.083523)
- Freedman, W. L. 2017, Nature Astron., 1, 0121, doi: [10.1038/s41550-017-0121](https://doi.org/10.1038/s41550-017-0121)
- Gelman, A., & Rubin, D. B. 1992, Statist. Sci., 7, 457, doi: [10.1214/ss/1177011136](https://doi.org/10.1214/ss/1177011136)
- Gogoi, A., Sharma, R. K., Chanda, P., & Das, S. 2021, Astrophys. J., 915, 132, doi: [10.3847/1538-4357/abfe5b](https://doi.org/10.3847/1538-4357/abfe5b)
- Hannestad, S. 2005, Phys. Rev. Lett., 95, 221301, doi: [10.1103/PhysRevLett.95.221301](https://doi.org/10.1103/PhysRevLett.95.221301)
- Hazra, D. K., Antony, A., & Shafieloo, A. 2022, <https://arxiv.org/abs/2201.12000>
- Heisenberg, L., Villarrubia-Rojo, H., & Zosso, J. 2022, arXiv e-prints, arXiv:2202.01202. <https://arxiv.org/abs/2202.01202>

- Heisenberg, L., Villarrubia-Rojo, H., & Zosso, J. 2022, <https://arxiv.org/abs/2201.11623>
- Heymans, C., et al. 2013, Mon. Not. Roy. Astron. Soc., 432, 2433, doi: [10.1093/mnras/stt601](https://doi.org/10.1093/mnras/stt601)
- Heymans, C., Tröster, T., Asgari, M., et al. 2021, A&A, 646, A140, doi: [10.1051/0004-6361/202039063](https://doi.org/10.1051/0004-6361/202039063)
- Hildebrandt, H., et al. 2020, Astron. Astrophys., 633, A69, doi: [10.1051/0004-6361/201834878](https://doi.org/10.1051/0004-6361/201834878)
- Jaber, M., & de la Macorra, A. 2018, Astropart. Phys., 97, 130, doi: [10.1016/j.astropartphys.2017.11.007](https://doi.org/10.1016/j.astropartphys.2017.11.007)
- James, F., & Roos, M. 1975, Computer Physics Communications, 10, 343, doi: [10.1016/0010-4655\(75\)90039-9](https://doi.org/10.1016/0010-4655(75)90039-9)
- Jassal, H. K., Bagla, J. S., & Padmanabhan, T. 2005, Phys. Rev. D, 72, 103503, doi: [10.1103/PhysRevD.72.103503](https://doi.org/10.1103/PhysRevD.72.103503)
- Jassal, H. K., Bagla, J. S., & Padmanabhan, T. 2010, MNRAS, 405, 2639, doi: [10.1111/j.1365-2966.2010.16647.x](https://doi.org/10.1111/j.1365-2966.2010.16647.x)
- Joudaki, S., et al. 2020, Astron. Astrophys., 638, L1, doi: [10.1051/0004-6361/201936154](https://doi.org/10.1051/0004-6361/201936154)
- Lemos, P., Lee, E., Efstathiou, G., & Gratton, S. 2019, MNRAS, 483, 4803, doi: [10.1093/mnras/sty3082](https://doi.org/10.1093/mnras/sty3082)
- Lewis, A., Challinor, A., & Lasenby, A. 2000, ApJ, 538, 473, doi: [10.1086/309179](https://doi.org/10.1086/309179)
- Li, X., & Shafieloo, A. 2019, Astrophys. J. Lett., 883, L3, doi: [10.3847/2041-8213/ab3e09](https://doi.org/10.3847/2041-8213/ab3e09)
- Linder, E. V. 2003, Phys. Rev. Lett., 90, 091301, doi: [10.1103/PhysRevLett.90.091301](https://doi.org/10.1103/PhysRevLett.90.091301)
- Linder, E. V. 2003, Physical Review Letters, 90, 091301, doi: [10.1103/PhysRevLett.90.091301](https://doi.org/10.1103/PhysRevLett.90.091301)
- Lorenz, C. S., Calabrese, E., & Alonso, D. 2017, Phys. Rev. D, 96, 043510, doi: [10.1103/PhysRevD.96.043510](https://doi.org/10.1103/PhysRevD.96.043510)
- MacCrann, N., Zuntz, J., Bridle, S., Jain, B., & Becker, M. R. 2015, Mon. Not. Roy. Astron. Soc., 451, 2877, doi: [10.1093/mnras/stv1154](https://doi.org/10.1093/mnras/stv1154)
- Marcondes, R. J. F., & Pan, S. 2017, <https://arxiv.org/abs/1711.06157>
- Martins, C. J. A. P., & Colomer, M. P. 2018, Astron. Astrophys., 616, A32, doi: [10.1051/0004-6361/201833313](https://doi.org/10.1051/0004-6361/201833313)
- Mawas, E., Street, L., Gass, R., & Wijewardhana, L. C. R. 2021, <https://arxiv.org/abs/2108.13317>
- Nojiri, S., Odintsov, S. D., & Oikonomou, V. K. 2017, Phys. Rept., 692, 1, doi: [10.1016/j.physrep.2017.06.001](https://doi.org/10.1016/j.physrep.2017.06.001)
- Nunes, R. C., & Vagnozzi, S. 2021, Mon. Not. Roy. Astron. Soc., 505, 5427, doi: [10.1093/mnras/stab1613](https://doi.org/10.1093/mnras/stab1613)
- Pandey, K. L., Karwal, T., & Das, S. 2020, J. Cosmology Astropart. Phys., 2020, 026, doi: [10.1088/1475-7516/2020/07/026](https://doi.org/10.1088/1475-7516/2020/07/026)
- Planck Collaboration, Aghanim, N., Akrami, Y., et al. 2020, A&A, 641, A6, doi: [10.1051/0004-6361/201833910](https://doi.org/10.1051/0004-6361/201833910)
- Poulin, V., Boddy, K. K., Bird, S., & Kamionkowski, M. 2018, Phys. Rev. D, 97, 123504, doi: [10.1103/PhysRevD.97.123504](https://doi.org/10.1103/PhysRevD.97.123504)
- Poulin, V., Boddy, K. K., Bird, S., & Kamionkowski, M. 2018, Phys. Rev. D, 97, 123504, doi: [10.1103/PhysRevD.97.123504](https://doi.org/10.1103/PhysRevD.97.123504)
- Poulin, V., Serpico, P. D., & Lesgourgues, J. 2016, JCAP, 08, 036, doi: [10.1088/1475-7516/2016/08/036](https://doi.org/10.1088/1475-7516/2016/08/036)
- Poulin, V., Smith, T. L., Karwal, T., & Kamionkowski, M. 2018, arXiv e-prints, arXiv:1811.04083, <https://arxiv.org/abs/1811.04083>
- Poulin, V., Smith, T. L., Karwal, T., & Kamionkowski, M. 2019, Phys. Rev. Lett., 122, 221301, doi: [10.1103/PhysRevLett.122.221301](https://doi.org/10.1103/PhysRevLett.122.221301)
- Riess, A. G., Casertano, S., Yuan, W., et al. 2021, Astrophys. J. Lett., 908, L6, doi: [10.3847/2041-8213/abdbaf](https://doi.org/10.3847/2041-8213/abdbaf)
- Riess, A. G., Casertano, S., Yuan, W., Macri, L. M., & Scolnic, D. 2019, ApJ, 876, 85, doi: [10.3847/1538-4357/ab1422](https://doi.org/10.3847/1538-4357/ab1422)
- Ross, A. J., Samushia, L., Howlett, C., et al. 2015, Mon. Not. Roy. Astron. Soc., 449, 835, doi: [10.1093/mnras/stv154](https://doi.org/10.1093/mnras/stv154)
- Roy, N., Goswami, S., & Das, S. 2022, <https://arxiv.org/abs/2201.09306>
- Sahni, V. 2002, Class. Quant. Grav., 19, 3435, doi: [10.1088/0264-9381/19/13/304](https://doi.org/10.1088/0264-9381/19/13/304)
- Schöneberg, N., Franco Abellán, G., Pérez Sánchez, A., et al. 2021, <https://arxiv.org/abs/2107.10291>
- Scolnic, D. M., et al. 2018, Astrophys. J., 859, 101, doi: [10.3847/1538-4357/aab9bb](https://doi.org/10.3847/1538-4357/aab9bb)
- Sutherland, W. 2018, MNRAS, 477, 1913, doi: [10.1093/mnras/sty687](https://doi.org/10.1093/mnras/sty687)
- Thejs Brinckmann, J. L. 2018, <https://arxiv.org/abs/1804.07261>
- Theodoropoulos, A., & Perivolaropoulos, L. 2021, Universe, 7, 300, doi: [10.3390/universe7080300](https://doi.org/10.3390/universe7080300)
- Vagnozzi, S. 2020, Phys. Rev. D, 102, 023518, doi: [10.1103/PhysRevD.102.023518](https://doi.org/10.1103/PhysRevD.102.023518)
- Vagnozzi, S., Dhawan, S., Gerbino, M., et al. 2018, Phys. Rev. D, 98, 083501, doi: [10.1103/PhysRevD.98.083501](https://doi.org/10.1103/PhysRevD.98.083501)
- Vagnozzi, S., Giusarma, E., Mena, O., et al. 2017, Phys. Rev. D, 96, 123503, doi: [10.1103/PhysRevD.96.123503](https://doi.org/10.1103/PhysRevD.96.123503)
- Visinelli, L., Vagnozzi, S., & Danielsson, U. 2019, Symmetry, 11, 1035, doi: [10.3390/sym11081035](https://doi.org/10.3390/sym11081035)
- Yang, W., Di Valentino, E., Pan, S., Shafieloo, A., & Li, X. 2021a, Phys. Rev. D, 104, 063521, doi: [10.1103/PhysRevD.104.063521](https://doi.org/10.1103/PhysRevD.104.063521)

Yang, W., Di Valentino, E., Pan, S., Wu, Y., & Lu, J.
2021b, Mon. Not. Roy. Astron. Soc., 501, 5845,
doi: [10.1093/mnras/staa3914](https://doi.org/10.1093/mnras/staa3914)

Zhang, Y.-C., Zhang, H.-Y., Wang, D.-D., et al. 2017,
Research in Astronomy and Astrophysics, 17, 050,
doi: [10.1088/1674-4527/17/6/50](https://doi.org/10.1088/1674-4527/17/6/50)

Zhao, G.-B., Raveri, M., Pogosian, L., et al. 2017, Nature
Astronomy, 1, 627, doi: [10.1038/s41550-017-0216-z](https://doi.org/10.1038/s41550-017-0216-z)

APPENDIX

A. EFFECT OF VARYING 4PDE EQUATION OF STATE PARAMETERS ON BAO AND SUPERNOVAE OBSERVABLES

The dark energy equation of state parameter w_0 is most sensitive to observables because it is equation of state when the dark energy density is dominating the universe. So an increase in the value of this parameter rapidly increase the dark energy density and the expansion rate of universe hence leave a major impact on the late time observables. This fact is evident from upper left panel of Figures 7, 8 and 9. The w_m parameter is the DE equation of state at earlier times. At that time the amount of the dark energy density was relatively less. So this equation of state parameters has less impact on the observables. The upper right panel of Figures 7, 8 and 9 show the impact of varying w_m on various observables. We can see that the change in the observables are relatively low in comparison to the case of parameter w_0 . The DE parameters a_t and Δ_{de} determine the width and the epoch of transition of the equation of state from w_m to w_0 . The effects of varying a_t and Δ_{de} are shown in the down-left and the down-right panels of the Figures 7, 8 and 9 respectively. We can see that parameter a_t has least impact on the observables given smooth (large width) transition preferred by the data. We also see that the DE parameter Δ_{de} has comparatively more impact on observables.

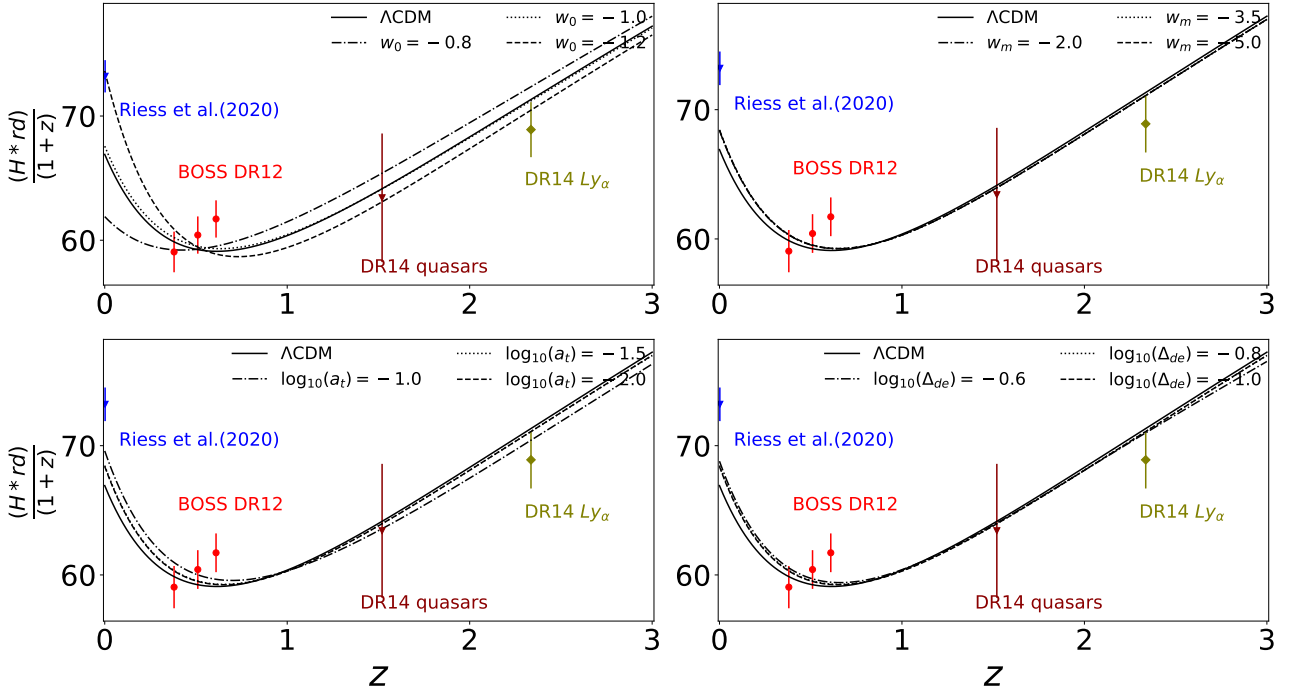


Figure 7. The plots of the evolution of $H(z)r_d/(1+z)$ for 4pDE models and reference ΛCDM model. Each of the four panels shows effect of varying different dark energy equation of state parameter (see the legends) while fixing other EoS parameters to values ($w_0 = -1.03$, $w_m = -3.97$, $\log_{10}(a_t) = -1.63$, $\log_{10}(\Delta_{de}) = -0.87$).

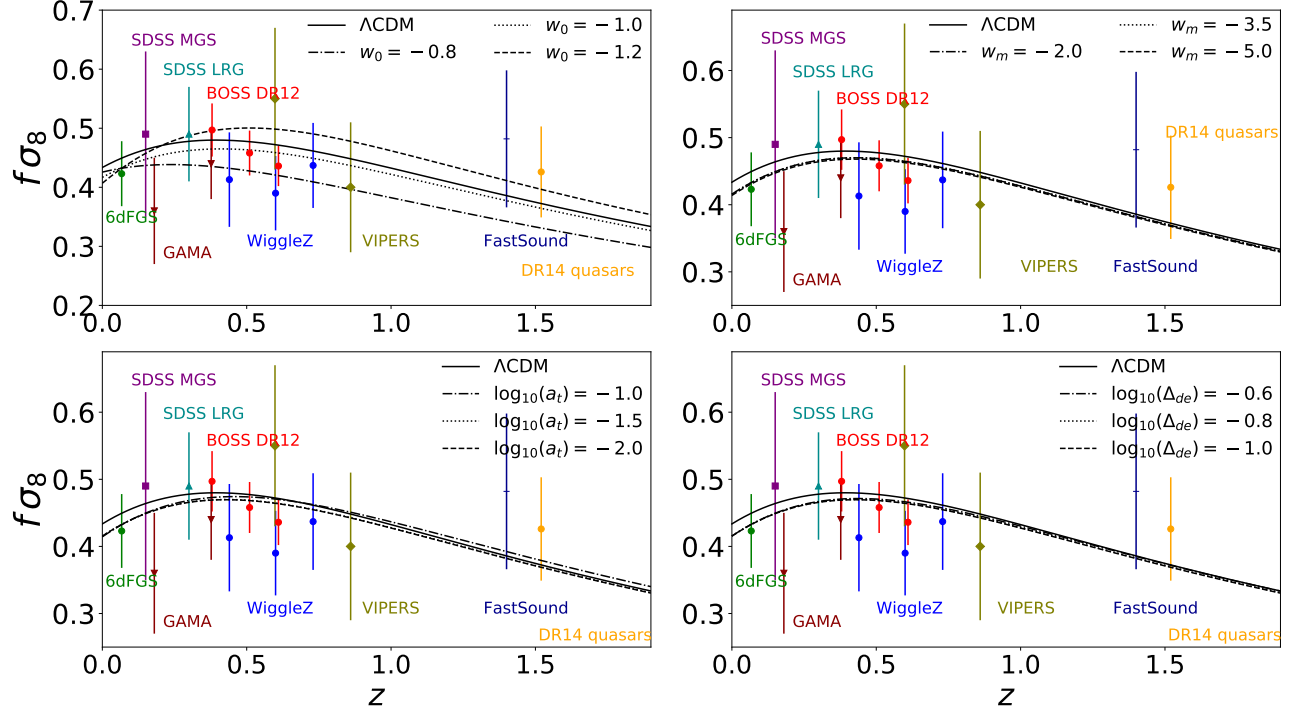


Figure 8. The plots of the evolution of the parameter $f\sigma_8$ as a function of redshift for 4pDE model and Λ CDM Model. Each of the four panels shows effect of varying different dark energy equation of state parameter (see the legends) while fixing other EoS parameters to values ($w_0 = -1.03$, $w_m = -3.97$, $\log_{10}(a_t) = -1.63$, $\log_{10}(\Delta_{de}) = -0.87$).

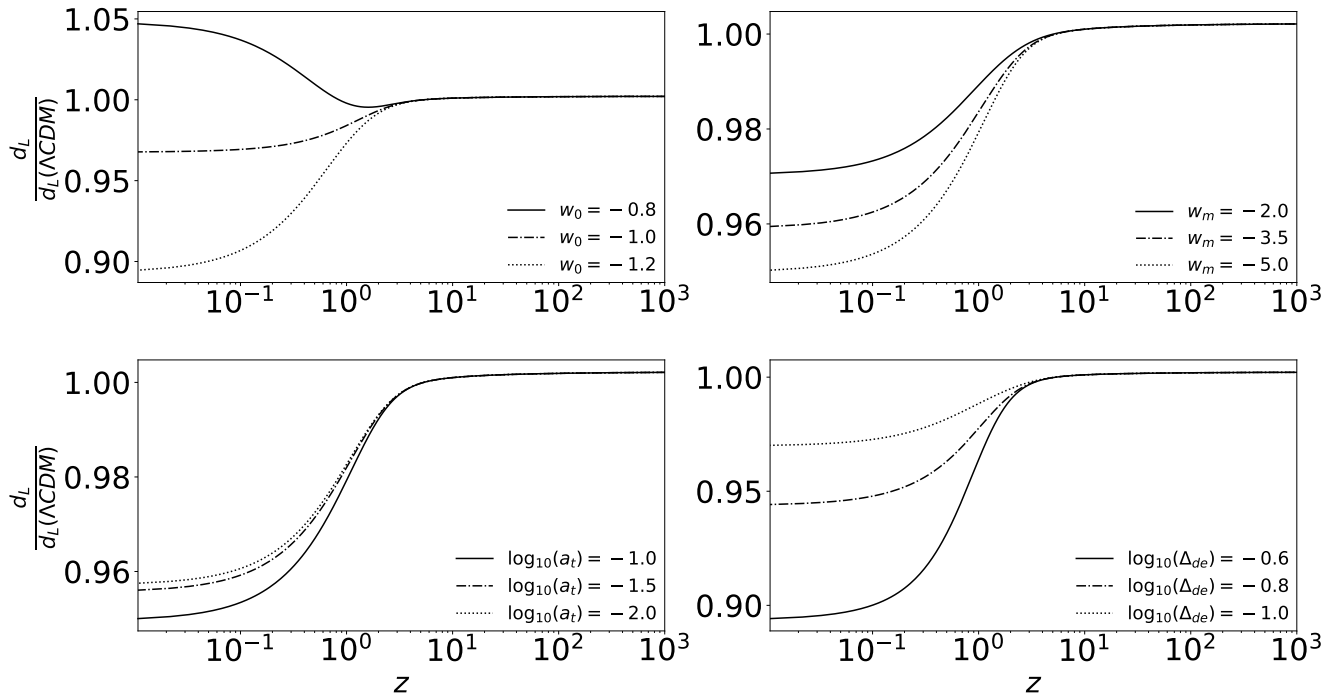


Figure 9. The plots of the evolution of the luminosity distance as a function of redshift for 4pDE model and Λ CDM model. Each of the four panels shows effect of varying different dark energy equation of state parameter (see the legends) while fixing other EoS parameters to values ($w_0 = -1.03$, $w_m = -3.97$, $\log_{10}(a_t) = -1.63$, $\log_{10}(\Delta_{de}) = -0.87$).